Virology 483 (2015) 275–283

Contents lists available at ScienceDirect

Virology

journal homepage: www.elsevier.com/locate/yviro

Complete genome sequence and integrated protein localization and interaction map for alfalfa dwarf virus, which combines properties of both cytoplasmic and nuclear plant rhabdoviruses

Nicolás Bejerman [a,b,*,1], Fabián Giolitti [a], Soledad de Breuil [a], Verónica Trucco [a], Claudia Nome [a], Sergio Lenardon [a], Ralf G. Dietzgen [b]

[a] Instituto de Patología Vegetal (IPAVE), Centro de Investigaciones Agropecuarias (CIAP), Instituto Nacional de Tecnología Agropecuaria (INTA), Camino a 60 Cuadras k 5,5, Córdoba X5020ICA, Argentina

[b] Queensland Alliance for Agriculture and Food Innovation, The University of Queensland, St Lucia, QLD 4072, Australia

ARTICLE INFO

Article history:
Received 15 March 2015
Returned to author for revisions
1 May 2015
Accepted 2 May 2015

Keywords::
Genome structure
Cytorhabdovirus
Nucleorhabdovirus
Protein localization
Protein–protein interactions
Phosphoprotein

SUMMARY

We have determined the full-length 14,491-nucleotide genome sequence of a new plant rhabdovirus, alfalfa dwarf virus (ADV). Seven open reading frames (ORFs) were identified in the antigenomic orientation of the negative-sense, single-stranded viral RNA, in the order 3′-N-P-P3-M-G-P6-L-5′. The ORFs are separated by conserved intergenic regions and the genome coding region is flanked by complementary 3′ leader and 5′ trailer sequences. Phylogenetic analysis of the nucleoprotein amino acid sequence indicated that this alfalfa-infecting rhabdovirus is related to viruses in the genus *Cytorhabdovirus*. When transiently expressed as GFP fusions in *Nicotiana benthamiana* leaves, most ADV proteins accumulated in the cell periphery, but unexpectedly P protein was localized exclusively in the nucleus. ADV P protein was shown to have a homotypic, and heterotypic nuclear interactions with N, P3 and M proteins by bimolecular fluorescence complementation. ADV appears unique in that it combines properties of both cytoplasmic and nuclear plant rhabdoviruses.

Introduction

In Argentina, alfalfa (*Medicago sativa* L.) is a primary forage crop and a major feed component in dairy and beef cattle production systems. In 2010, a rhabdovirus was found associated with alfalfa plants showing symptoms of shortened internodes (bushy appearance), leaf puckering and varying-sized vein enations on abaxial leaf surfaces (Bejerman et al., 2011). The plants that showed these distinct symptoms were diagnosed as being co-infected by a rhabdovirus and alfalfa mosaic virus (AMV), led to significant yield losses and reduced the useful economic life of the crop (Trucco et al., 2014). Alfalfa dwarf disease had a prevalence of over 70% in several growing regions of Argentina and preliminary evaluations showed yield reductions of up to 30% (S. Lenardon, pers. comm.).

Members of the family *Rhabdoviridae* can infect a wide range of hosts, including humans, livestock, fish, plants, and insects (Ammar et al., 2009; Jackson et al., 2005; Kuzmin et al., 2009). Six rhabdovirus genera are recognized by the International Committee on Taxonomy of Viruses (ICTV) in its 9th report (Dietzgen et al., 2011) and five additional genera have since been approved (ICTV Master Species List 2013v2). Plant-infecting rhabdoviruses are currently classified into two genera, *Nucleorhabdovirus* and *Cytorhabdovirus,* which are distinguished depending on whether the viruses elicit inclusions in the nucleus, bud from the inner nuclear envelope, and accumulate in perinuclear spaces, or whether they develop cytoplasmic viroplasms, undergo morphogenesis from cytoplasmic membranes, and accumulate in the cytoplasm, respectively (Jackson et al., 2005). Viruses of both genera are transmitted by insects, in which they also replicate and circulate. Plant rhabdoviruses have been reported worldwide, and can infect most major crops and a number of weed hosts in temperate, subtropical and tropical regions (Jackson et al., 2005; Redinbaugh and Hogenhout, 2005).

Plant rhabdoviruses have non-segmented negative-sense, single stranded RNA genomes of approximately 11–15 kb, that encode at least six proteins: nucleocapsid protein (N), phosphoprotein (P), movement protein (P3), matrix protein (M), glycoprotein (G) and RNA-dependent RNA polymerase (L) in the order 3′ N-P-P3-M-G-L 5′ (Dietzgen et al., 2011). The viral RNA is tightly encapsulated by the N protein, and this N-RNA complex, together with the P and L

* Corresponding author at: Instituto de Patología Vegetal (IPAVE), Centro de Investigaciones Agropecuarias (CIAP) Instituto Nacional de Tecnología Agropecuaria (INTA), Camino a 60 Cuadras k 5,5, Cordoba X5020ICA, Argentina. Tel.: +54 351 4973636.

E-mail addresses: n.bejerman@uq.edu.au, nicobejerman@gmail.com (N. Bejerman).

[1] Present address: Queensland Alliance for Agriculture and Food Innovation, The University of Queensland, St Lucia, QLD 4072, Australia. Tel.: +61 7 3346 6521.

http://dx.doi.org/10.1016/j.virol.2015.05.001
0042-6822/

proteins, forms a helical ribonucleoprotein (RNP) complex that is essential for virus replication. The M protein is thought to be responsible for condensation of RNP complexes into a skeleton-like structure (RNP-M core) during virion assembly, and G protein is thought to form trans-membrane spikes (Jackson et al., 2005).

Although more than 75 plant rhabdoviruses have been detected in a variety of host species based on their large bacilliform virions, the complete genome sequences of only 6 cytorhabdoviruses (Dietzgen et al., 2006; Heim et al., 2008; Ito et al., 2013; Schoen et al., 2004; Tanno et al., 2000; Yan et al., 2015) and 8 nucleorhabdoviruses (Bandyopadhyay et al., 2010; Heaton et al., 1989; Huang et al., 2003; Massah et al., 2008; Pappi et al., 2013; Reed et al., 2005; Revill et al., 2005; Tsai et al., 2005) have been determined. Thus, the sequence determination of the complete genomes of additional plant rhabdoviruses is sorely needed to support and clarify the taxonomy of this important group of viruses and lead to a better understanding of their evolutionary trajectories.

Initial electron microscopy and phylogenetic analysis of a partial fragment of the L gene suggested that the alfalfa-infecting rhabdovirus is a tentative member of the genus *Cytorhabdovirus*, which has been named alfalfa dwarf virus (ADV) (Bejerman et al., 2011). Here, we report and analyze the complete genome sequence of ADV, demonstrate the intracellular localization of its encoded proteins by transient expression as autofluorescent fusions in *Nicotiana benthamiana* leaves and establish a viral protein–protein interaction map. Unexpectedly, viral protein localization and interactions were not fully consistent with ADV being a cytorhabdovirus, whereas these properties have been in complete agreement for all other plant rhabdoviruses analyzed so far.

Results

Alfalfa dwarf virus genome sequence analysis

The negative-sense RNA genome of ADV is 14,491 nucleotides (nt) in length (GenBank accession number KP205452) and contains seven open reading frames (ORFs) in the anti-genome, positive-sense orientation (Fig. 1B). BlastX searches identified these ORFs as encoding the nucleocapsid protein (N; ORF1), phosphoprotein (P; ORF2), putative movement protein (P3; ORF3), matrix protein (M; ORF 4), glycoprotein (G; ORF 5), and RNA-dependent RNA polymerase (L; ORF 7) based on highest sequence identity scores with plant rhabdoviruses, whereas P6 (ORF6) did not have significant matches with any Genbank plant rhabdovirus entries (Table 1). The coding sequences are flanked by complementary 3′ leader (l) and 5′ trailer (t) sequences (the 22 terminal nt are complementary) revealing a genome organization of 3′ l-N-P-P3-M-G-P6-L-t 5′ (Fig. 1B). All ADV genes are separated by conserved gene junctions, which are composed of a polyadenyilation signal of the preceding gene, an intergenic region which varied in length from 3 nt to 18 nt, and a transcriptional start of the following gene (Table 2). ADV gene junctions were most similar to those of cytorhabdoviruses (Table 2). Amino acid (aa) sequence comparisons between the deduced ADV proteins (except P protein) and the corresponding sequences of other plant rhabdoviruses (Table 3) revealed the closest relationships to cytorhabdoviruses, in particular persimmon virus A (PeVA) (the full genome data for strawberry crinkle virus (SCV) is not accessible). However, ADV P protein shared similar sequence identities with both cyto- and nucleorhabdoviruses (Table 3). The levels of amino acid sequence identity between ADV and PeVA were low and ranged from 17.4% in the matrix proteins to 43.1% in the L polymerase proteins; ADV M protein was most similar to the M protein of lettuce yellow mottle virus (LYMoV) (Table 3).

The characteristics of proteins encoded by ADV genome as determined by predictive algorithms are shown in Table 1. The N gene contains a 1443-nt ORF, which encodes the nucleocapsid protein with predicted molecular weight of 53.2 kDa and an isoelectric point of 9.07; sequence identity between the N proteins of ADV and other cytorhabdoviruses ranged from 19.9% to 31.4% (Table 3). The P gene contains a 933-nt ORF, which encodes the phosphoprotein with a predicted molecular weight of 35.1 kDa and an isoelectric point of 4.68; sequence identity between the P proteins of ADV and other cytorhabdoviruses ranged from 14.7% to 19.7% (Table 3). The P3 gene contains a 720-nt ORF, which encodes the putative movement protein with a predicted molecular weight of 27 kDa and an isoelectric point of 9.92; sequence identity between the P3 proteins of ADV and other cytorhabdoviruses ranged from 14.7% to 18.5% (Table 3). The M gene contains a 570-nt ORF, which encodes the putative matrix protein with a predicted molecular weight of 20.4 kDa and an isoelectric point of 8.05; sequence identity between the M proteins of ADV and other cytorhabdoviruses ranged from 17.4% to 22.7% (Table 3).

The G gene contains a 1692-nt ORF, which encodes the glycoprotein with a predicted molecular weight of 63.05 kDa and an isoelectric point of 7.7; the sequence identity between the G proteins of ADV and other cytorhabdoviruses ranged from 19.4% to 29.5% (Table 3). The amino terminal region of the ADV G protein is hydrophobic, and its overall hydrophilicity plot (data not shown) is similar to those of the G proteins of LYMoV (Heim et al., 2008) and lettuce necrotic yellows virus (LNYV) (Dietzgen et al., 2006). In ADV G, a signal peptide consisting of 30 aa and containing a IGD=R (=indicates the predicted cleavage site) was identified. Additionally, six potential glycosylation sites (N-[P]-S/T-[P]-) were

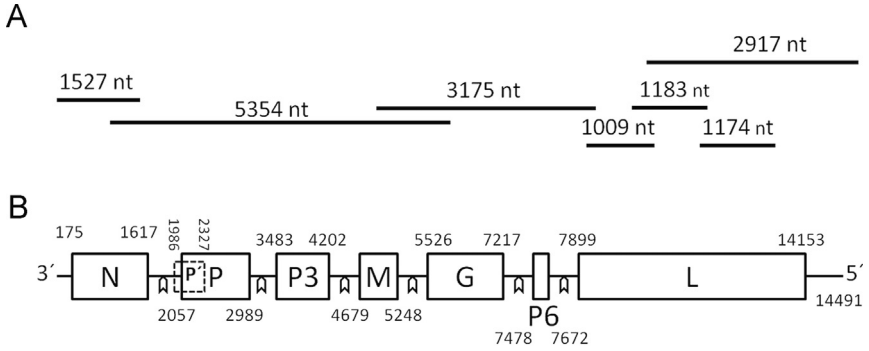

Fig. 1. Schematic diagram of ADV (A) genome sequencing strategy and (B) genome organization. The seven overlapping fragments amplified to cover the whole genome are indicated in (A). Open reading frames (ORFs) are shown as squares and N, P, P3, M, G, P6, L genes identified in (B). Numbers above or below each ORF, indicate ORF first and last nucleotides. Intergenic regions are indicated by arrowheads and the internal P gene ORF P′ is shown as dashed square.

Table 1
Characteristics of proteins encoded by alfalfa dwarf virus genome determined by predictive algorithms.

ORF No.[a]	Gene name	Calculated *Mr* (kDa)	isolelectric point	Putative function	Predicted NLS	TM	Highest scoring virus protein/*E*-value (Blast X)
1	N	53.21	9.07	Nucleocapsid	None	None	LNYV N/3e-55
2	P	35.12	4.68	Phosphoprotein	None	None	PeVA P/5e-04
3	P3	27.03	9.92	Movement	None	None	PeVA P3/0.027
4	M	20.40	8.05	Matrix protein	None	None	LYMoV M/0.003
5	G	63.05	7.70	Glycoprotein	None	aa 508–530	PeVA G/1e-65
6	P6	7.60	9.14	Unknown	None	aa 31–50	Not significant
7	L	237.68	8.25	Polymerase	None	None	PeVA L/0.0

TM=Transmembrane domain; NLS=nuclear localization signal.

[a] ORF numbers are represented from 3′ to 5′ for genomic sense and correspond to those in Fig.1B. The overlapping ORF P′ is not shown in the Table.

Table 2
Gene junction regions of Alfalfa dwarf virus and other selected plant rhabdoviruses.

ADV	Gene end	Intergenic sequence	Gene start
I/N		GAUGGCUCUAUGACU	CUU
N/P	CCAAAUUAUUUU	GAU	CUU
P/3	CCAAAUUAUUUU	GAUCGAGCUAU	CUU
3/M	CCAAAUUAUUUU	GAUACGUUAG	CUU
M/G	CCAAUUUAUUUU	GAUC	CUU
G/6	CCAAAUUAUUUU	GAUAUCCGUUACGUUUAU	CUU
6/L	CCAAAAUUGUUU	GAUACUCUCGUC	CUU
consensus	CCAAAUUAUUUU	GAU	CUU
PeVA	AUUNUUUU	GNU(N)n	UUU
LNYV	AUUCUUUU	G(N)n	CUU
LYMoV	AUUCUUUU	G(N)n	CUN
NCMV	AUUCUUUUU	GACU	CUA
BYSMV	AUUAUUUUU	GA	CUC
RYSV	AUUCUUUUU	GGG	UUG
PYDV	AUUAUUUUU	GGG	UUG
SYNV	AUUCUUUUU	GG	UUG

ADV consensus sequences are highlighted in gray. For virus acronyms and GenBank accession numbers see legend to Fig.2.

Table 3
Amino acid sequence identities (%) of alfalfa dwarf virus proteins compared with those of other cytorhabdoviruses and selected nucleorhabdoviruses.

	N	P	P3	M	G	P6	L
PeVA	31.4	19.7	18.5	17.4	29.5	–	43.1
LNYV	28.1	19.0	15.4	19.0	27.8	–	38.6
LYMoV	30.4	16.4	14.7	22.7	26.4	–	40.4
NCMV	20.7	14.7	16.0	18.5	20.3	–	29.1
BYSMV	19.9	19.1	15.0	20.6	19.4	–	28.6
RYSV	16.2	18.1	8.7	12.9	15.4	6.9	23.1
SYNV	16.9	17.5	11.9	9.0	16.8	–	24.1
PYDV	16.4	16.9	10.8	10.8	14.2	–	22.2

For virus acronyms and GenBank accession numbers see legend to Fig. 2.

predicted in the mature G protein of ADV, compared to four for LYMoV and three for LNYV G protein. Furthermore, a transmembrane domain was identified in the C-terminal region (aa positions 508–530) (Table 1). Similar domains were also reported in this region for other plant rhabdoviruses (Bandyopadhyay et al., 2010; Dietzgen et al., 2006; Heim et al., 2008).

A small ORF, which encodes a protein of unknown function named P6 was identified between G and L coding regions. P6 gene contains a 195-nt OFR with a predicted molecular weight of 7.6 kDa and an isoelectric point of 9.14. The L gene contains a 6255-nt ORF, which encodes a protein with a predicted molecular weight of 237.7 kDa and an isoelectric point of 8.25. The L protein of ADV contained motifs characteristic of RNA-dependent RNA polymerases of negative-strand RNA viruses (Bourhy et al., 2005). The similarity between the L proteins of different plant rhabdoviruses is highest in domain III, which includes the motif GDN, thought to represent the catalytic center (Dietzgen et al., 2006). Sequence identity between the L proteins of ADV and other cytorhabdoviruses ranged from 28.6% to 43.1% (Table 3). Overall, ADV L protein was the most conserved of the viral proteins. One additional overlapping ORF was found in the ADV genome. This ORF occurs in an overlapping +1 reading frame within the P gene (P′), located between nucleotides 1986 and 2327 (Fig. 1B), and potentially encoding a protein of 13.8 kDa. A similar ORF was found in the P genes of northern cereal mosaic virus (NCMV), LNYV and LYMoV (Dietzgen et al., 2006; Heim et al., 2008; Tanno et al., 2000). Database searches using BlastP did not reveal any significant similarities with other proteins.

We previously used a 1 kb fragment of the L gene to show that ADV is most closely related to viruses in the genus *Cytorhabdovirus* (Bejerman et al., 2011). Here, we use the deduced aa sequence of the N protein and the domain III of the L protein in phylogenetic analyses using the neighbor-joining (NJ) (Fig. 2) and maximum likelihood (ML) (data not shown) methods to confirm that ADV clusters with the cytorhabdoviruses (Fig. 2A), and that ADV is most closely related to SCV and raspberry vein chlorosis virus (RVCV) (Fig. 2B). Furthermore, both phylogenetic trees show two clades of cytorhabdoviruses, one that includes all dicot-infecting viruses and another containing two monocot-infecting viruses (Fig. 2A and B). In the genomes of the latter group (BYSMV and NCMV), multiple transcriptional units are present between the P and M genes, distinct from the genome organization of ADV and other sequenced dicot cytorhabdoviruses.

Subcellular localization of ADV proteins

Viral protein localization in host cells provides valuable information about viral replication and assembly sites (Martin et al., 2012). However, subcellular localization of viral proteins is difficult to determine solely from *in silico* predictions (Bandyopadhyay et al., 2010). Therefore, we transiently expressed individual ADV proteins as fusions to the C-terminus or N-terminus of green fluorescent protein (GFP) to visualize intracellular localization by live cell imaging using confocal laser scanning microscopy. To assist in identification of intracellular structures, endoplasmic reticulum (ER)-targeted mCherry marker was co-infiltrated with GFP fusion constructs (Fig. S1) or transgenic fluorescent nuclear marker plants expressing red fluorescent protein (RFP)-fused to histone 2B were used (Fig. 3A).

GFP-N uniformly co-localized with the mCherry-ER marker on nuclear membranes and the cell periphery frequently as small aggregates (Fig. 3A and Fig. S1). When ADV N was expressed as fusion to the N-terminus of GFP, the localization was similar (data not shown). Surprisingly, GFP-P localized exclusively to a well-defined area within the cell nucleus (Fig. 3A and Fig. S1), despite a lack of predictable nuclear localization signals (NLSs) using conventional protein domain algorithms; furthermore no nuclear export signal was predicted when this protein was analyzed using NetNES (data not shown). ADV P protein localization resembled

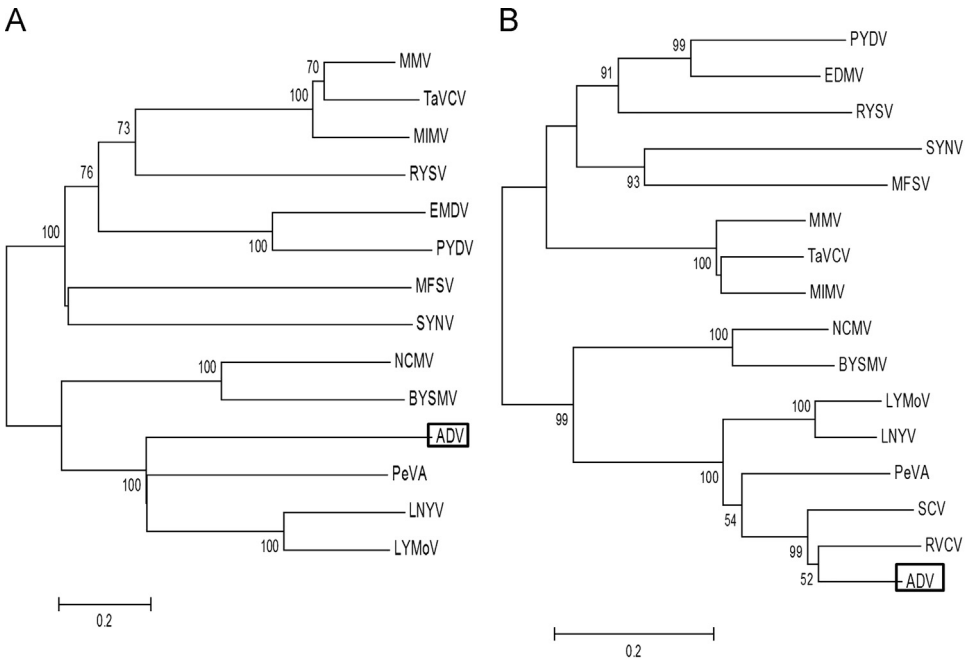

Fig. 2. Neighbor-joining phylogenetic trees showing relationship of the amino acid sequences of the nucleocapsid protein (A) and domain III of the polymerase protein (B) of ADV and corresponding sequences of other plant rhabdoviruses. The viruses and their accession numbers are: barley yellow striate mosaic virus (BYSMV; KM213865), eggplant mottled dwarf virus (EDMV; NC_025389), lettuce yellow mottle virus (LYMoV; EF687738), lettuce necrotic yellows virus (LNYV; NC_007642); maize fine streak virus (MFSV; AY618417), maize Iranian mosaic virus (MIMV; DQ186554), maize mosaic virus (MMV; AY618418), northern cereal mosaic virus (NCMV; NC_002251), persimmon virus A (PeVA; NC_018381), potato yellow dwarf virus (PYDV; GU734660), raspberry vein chlorosis virus (RVCV; FN812699), rice yellow stunt virus (RYSV; NC_003746); sonchus yellow net virus (SYNV; L32603), strawberry crinkle virus (SCV; AY250986), taro vein chlorosis virus (TaVCV; AY674964). Bootstrap values of 1000 replicates are indicated at the branch points. The scale bar indicates substitutions per amino acid site.

that of a nuclear viroplasm and resulted in the compression of host DNA associated with H2B to the periphery of the nucleus with a red ring-like appearance (Fig. 3A). On the other hand, when ADV P was fused to the N-terminus of GFP, only a weak fluorescent signal was observed and protein localization could not be clearly determined.

When RFP-N was co-expressed with GFP-P, the majority of both proteins co-localized in the nucleus and N protein in the cell periphery was significantly reduced (Fig. 3B), suggesting an interaction between ADV N and P proteins leading to import of additional N protein into the nucleus.

GFP-P3 (Fig. 3A and Fig. S1) and P3-GFP (data not shown) localized mostly to the cell periphery, but were also seen in the nucleus. GFP-M and GFP-P6 localized in both the nucleus and cell periphery (Fig. 3A and Fig. S1), while GFP-G was found exclusively in nuclear membranes and the ER (Fig. 3A and Fig. S1). The N-terminal GFP fusions M-GFP, P6-GFP and G-GFP showed intracellular localizations similar to their C-terminal fusion counterparts (data not shown). When RFP-M was co-expressed with GFP-P, the majority of both proteins co-localized in a well-defined area within the cell nucleus and M protein in the cell periphery was significantly reduced (Fig. 3B), suggesting an interaction between ADV M and P proteins leading to import of additional M protein into the nucleus.

Interaction matrix for ADV proteins

Bimolecular fluorescence complementation (BiFC) was used to determine the binary interactions and localization patterns of ADV proteins N, P, P3, M, G and P6 in all pair-wise combinations and with glutathione-S-transferase (GST), which served as a non-binding control (Fig. 4A). The L protein was not included in these experiments due to the inability to stably express this 237 kDa protein *in planta*. None of the ADV proteins showed any interaction with GST in either of the reciprocal fusions. Therefore, we show only one example of these control experiments (Fig. 4). Positive BiFC interactions were detected (as restored YFP fluorescence) for N:P, P:P, P3:P and M:P in both orientations using the C1 BiFC vectors (Fig. 4). The only homotypic self-interaction detected by BiFC was that of P protein. The heterotypic interactions of ADV P protein with N, P3 and M resulted in the punctuate intranuclear accumulation of these viral protein complexes (Fig. 4A). While N:P and P3:P complexes had an irregular distribution across the nucleus, M:P punctate complexes localized chiefly in the nuclear periphery, which may indicate that the cell nucleus is a focal point for ADV replication machinery and viroplasm establishment. Furthermore, as shown in Fig. 4A, M:P interaction influenced host DNA localization. It appears that these protein interactions with ADV P resulted in the relocalization of N, P3 and M to the nucleus (compare Figs. 3A and 4A). In all other pairwise combinations of ADV proteins tested no interactions were detected (data not shown). The results of the BiFC experiments were used to generate a diagrammatic map of protein interactions and localization for ADV (Fig. 4B).

Co-expression of N or M proteins with P (Fig. 3B) showed a sub-nuclear co-localization similar to the N:P and M:P interactions observed by BiFC (Fig. 4A). However, in contrast to the sub-nuclear P3:P interaction seen in BiFC experiments (Fig. 4A), co-expression of P and P3 resulted in only a partial co-localization of the two proteins and sub-nuclear re-localization of P3; a significant proportion of RFP-P3 remained localized in the cell periphery (compare Fig. 3A and B).

Discussion

ADV has been proposed as representative of a tentative new species in the genus *Cytorhabdovirus*, family *Rhabdoviridae* based on the phylogenetic analysis of partial L gene sequence (Bejerman et al., 2011). In this current report we have determined the

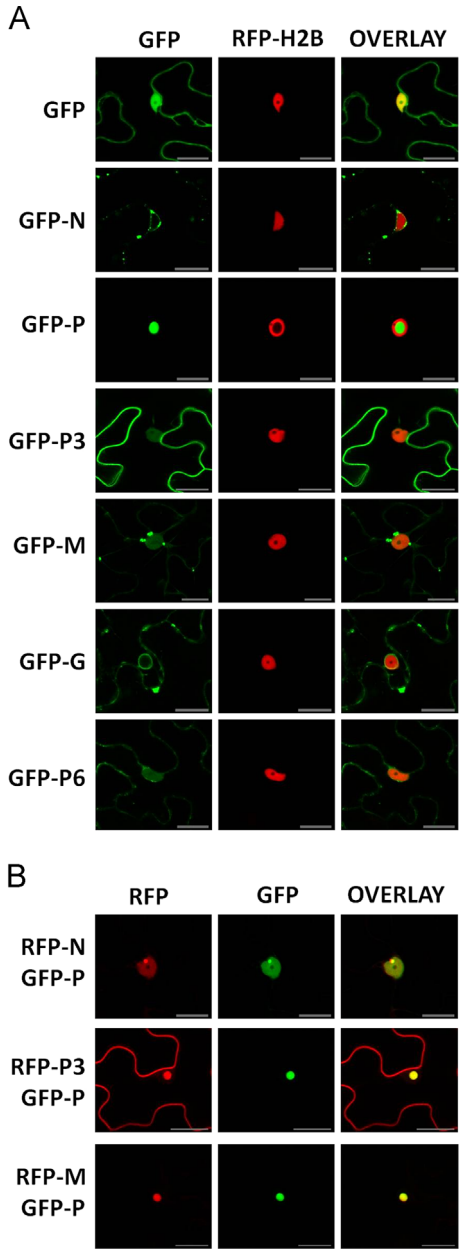

Fig. 3. Intracellular localization of transiently expressed ADV proteins. Green fluorescent protein (GFP) fusions to ADV N, P, P3, M, G and P6 proteins were individually expressed from pSITE-2CA vector in agroinfiltrated *Nicotiana benthamiana* epidermal leaf cells and confocal laser scanning microscope images taken after 2–3 days. Cultures of transformed Agrobacterium harboring ADV constructs were infiltrated into transgenic red fluorescent protein-Histone 2B marker plants (A). The left panel shows GFP-fusions, middle panel red intracellular marker, and right panel the merged images of both channels. (B) shows co-expression of RFP-N and GFP-P (top row), RFP-P3 and GFP-P (middle row) and RFP-M and GFP-P (bottom row). Experiments were repeated 3 times and a minimum of 50 cells viewed per construct. Scale bar represents 20 μM.

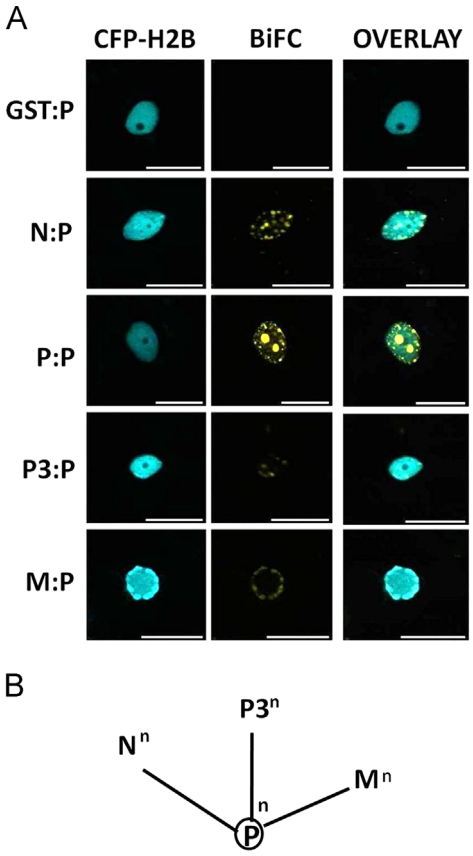

Fig. 4. Confocal micrographs showing ADV protein–protein interactions determined by bimolecular fluorescence complementation. Interaction assays were conducted in leaf epidermal cells of transgenic *Nicotiana benthamiana* expressing cyan fluorescent protein fused to the nuclear marker histone 2B (CFP-H2B). Shown are the localization of CFP-H2B (nucleus, column 1), interaction assay (BiFC, column 2), and a merge of the two preceding panels (overlay, column 3). Proteins listed first in the pair of interactors were expressed as fusions to the amino-terminal half of yellow fluorescent protein (YFP). Those listed second were expressed as fusions to the carboxy-terminal half of YFP. However, protein fusions to each half of YFP were tested in all pairwise combinations, of which a subset is shown here. Representative results using glutathione-S transferase (GST) fusions as non-binding negative controls with the ADV interactors are shown as GST-P. Experiments were repeated 3 times and a minimum of 50 cells viewed per construct. Scale bar represents 20 μM (A). Schematic diagrams of the viral protein–protein interaction and localization maps for ADV (B). Self-interactions are indicated by a circle. Lines indicate heterologous interactions. Superscripts indicate subcellular localization: *n*=nucleus.

complete ADV genome sequence of 14,491 nt and analyzed its coding and intergenic regions. The taxonomic classification of ADV as cytorhabdovirus was supported by phylogenetic analysis of the aa sequences of the N protein and domain III of L protein, which show a close evolutionary relationship of ADV with the cytorhabdoviruses SCV and PeVA. SCV has a slightly larger genome composed of 14,547 nt, but with the same genome organization as ADV (Schoen et al., 2004); therefore ADV and SCV may have shared a common ancestor. As is typical for all rhabdoviruses the 3′ leader and 5′ trailer sequences are complementary and capable of forming a putative panhandle structure thought to be involved in genome replication. The degree of complementarity found between 3′leader and 5′trailer sequences for ADV (22/22) is the highest within the cytorhabdoviruses (17/20 for PeVA, 22/25 for LYMoV, 19/25 for LNYV and 13/20 for NCMV). Furthermore, no unmatched base overhangs were observed in the aligned leader sequence of ADV whereas overhangs in the leader sequences have been reported for cytorhabdovirus genomes PeVA (Ito et al., 2013), LYMoV (Heim et al., 2008), LNYV (Dietzgen et al., 2006) and NCMV (Tanno et al., 2000); nevertheless the significance of this finding regarding potential influence on the virus life cycle is unknown. As is the case for all plant rhabdoviruses, ADV genes are separated by intergenic "gene junction" regions that are highly conserved but slightly divergent from those reported for the other plant rhabdoviruses. ADV ORF sequences, except M, are most similar to their respective counterparts in PeVA; however the highest amino acid sequence identity is only 43.1% between the L proteins. Unfortunately, we could not compare the ADV proteins with those of SCV, because the genome sequence of SCV is not publically available although it has been reported as completed (Schoen et al., 2004).

This low level of sequence identity is typical of both the cyto- and nucleorhabdoviruses characterized so far, all of which appear highly diverse, both in sequence of encoded proteins and in genome organization (Jackson et al., 2005; Walker et al., 2011). Furthermore, an accessory gene, which encodes a protein named P6, was identified in ADV between the G and L protein coding regions. ADV is only the fifth plant rhabdovirus, which has an accessory gene in this position. ADV P6 gene contains a 195-nt ORF whereas SCV P6 ORF is 9 nt longer (Schoen et al., 2004), while NCMV P9 ORF is 39 nt shorter (Tanno et al., 2000) and barley yellow striate mosaic virus (BYSMV) P9 ORF is 42 nt shorter (Yan et al., 2015). An accessory ORF in this position was also identified and characterized for the nucleorhabdovirus rice yellow stunt virus (RYSV) (Huang et al., 2003). RYSV P6 ORF is 84 nt longer than ADV P6 and functions as suppressor of systemic RNA silencing (Guo et al., 2013). However, ADV and SCV P6, BYSMV P9 and NCMV P9 are basic proteins, whereas RSYV P6 is highly acidic (Huang et al., 2003). No sequence homology is evident between any of these proteins.

To further characterize the encoded proteins of ADV genome, we investigated their subcellular localization and interactions *in planta*. The protein localization and interactome of the *Cytorhabdovirus* type species LNYV was recently reported (Martin et al., 2012). This study is the second report of the localization and interactions of proteins for a cytorhabdovirus, and the first such study for a cytorhabdovirus P6 accessory protein.

ADV N protein localized to the cell periphery and nuclear membrane, which is similar to the localization reported for LNYV N (Martin et al., 2012). Both ADV P3 and M localized to the cell periphery and the nuclei, however LNYV 4b (putative cell-to-cell movement protein and P3 homolog according to the genome organization) showed a stronger nuclear localization (Martin et al., 2012) compared with that of ADV P3. This was supported by a predicted NLS in LNYV 4b C-terminal domain, whereas no canonical NLS was predicted for ADV P3. ADV M localization was similar to that reported for LNVY M (Martin et al., 2012). The G protein of ADV was exclusively localized to nuclear and ER membranes when transiently expressed in *N. benthamiana* epidermal leaf cells, similar to LNYV G (Martin et al., 2012). This localization agrees with the predicted membrane association of G protein spikes in assembled virus particles (Jackson et al., 2005). Localization of ADV P6 protein in the cell periphery and the nucleus is similar to that reported for RYSV P6 (Guo et al., 2013), but different to that reported for BYSMV P9, which was localized in the cell periphery and nuclear membranes but not in the nucleus (Yan et al., 2015).

Although no NLS could be identified using current predictive computational methods, ADV P fusion protein was targeted exclusively to the nucleus, when its amino terminus was fused to the carboxy terminus of GFP. This nuclear localization of ADV P differed from the cytoplasmic localization observed for the cytorhabdovirus LNYV P (Martin et al., 2012), but was similar to that seen for potato yellow dwarf nucleorhabdovirus (PYDV) P which is exclusively nuclear, despite lacking predicted canonical NLSs (Ghosh et al., 2008). On the other hand, when the carboxy terminus of ADV P was fused to the amino terminus of GFP, only a weak fluorescent signal was observed and protein intracellular localization could not be clearly determined. This suggests a binding domain in the C-terminus of P protein that may be required for localization and movement into the nucleus; this binding domain may be blocked by the fusion to GFP in that location. The effect of the autofluorescent proteins on the stability and expression of fusion proteins has been previously reported for other proteins (Goodin et al., 2007). The lack of a canonical NLS for ADV P using predictive algorithms agrees with findings by Anderson et al. (2012) who postulated that current computational methods likely underestimate the number of proteins targeted to the nucleus because algorithms used to predict nuclear localization are designed primarily based on basic, arginine/lysine-rich regions, typical of proteins imported into the nucleus by importin α/β-mediated pathways (Cokol et al., 2000). However, many novel non-basic NLSs are emerging that are not detected using the most popular predictive algorithms (Kumar and Raghava, 2009; Mattaj and Englmeier, 1998). Furthermore, it was demonstrated that neither SYNV P (Deng et al., 2007; Martin et al., 2009) nor PYDV P (Martin et al., 2009) interact with importin-α prompting us to speculate that ADV P may utilize a similar nuclear import pathway alternative to the one mediated by importin α/β.

In all rhabdoviruses where viral protein localizations have been studied, the co-expression of N and P proteins have altered their individual localization patterns relative to when they are expressed alone. It has been demonstrated that cytorhabdovirus N and P proteins can co-localize and interact to form aggregates in the cytoplasm near the nucleus (Martin et al., 2012) and nucleorhabdovirus N and P proteins interact inside the nucleus (Ghosh et al., 2008; Goodin et al., 2001, 2002; Tsai et al., 2005). Despite having close evolutionary ties with cytorhabdoviruses based on phylogenetic analyses, based on our co-localization and interaction studies, ADV N and P proteins behave more like their nucleorhabdovirus counterparts. Co-expression of ADV N and P led to a near-exclusive co-localization across the nucleus (excluding the nucleolus), whereas co-expressed SYNV N and P proteins shift to a sub-nuclear location, distinct from the nucleolus (Goodin et al., 2001, 2002). In contrast, maize fine streak virus (MFSV) and PYDV N and P proteins co-localize in the nucleolus (Ghosh et al., 2008; Tsai et al., 2005). In the case of the nucleorhabdoviruses SYNV and MFSV the N-P co-expression leads to an import of P to the nucleus (Goodin et al., 2001; Tsai et al., 2005), whereas in the cytorhabdovirus LNYV cytoplasmic viroplasm-like aggregates formed (Martin et al., 2012). On the other hand, ADV N and P protein co-expression led to an increased import of N protein to the nucleus, although cytorhabdoviruses, unlike nucleorhabdoviruses, have been shown to lack an intimate association with the nucleus and nuclear membranes (Jackson et al., 2005). The nuclear localization of the ADV N:P complex, which together with L protein form the nucleocapsid core for genome replication and mRNA synthesis may indicate different infection mechanism and replication site for ADV and LYNV. It is tempting to hypothesize that the formation of the virus replication factory for ADV may require nuclear accumulation of both the N and P proteins mediated by P protein acting as a nuclear import shuttle for cognate N protein.

A BiFC interaction map for ADV proteins was constructed because it provides simultaneous interaction and localization data *in planta* (Citovsky et al., 2006; Martin et al., 2009). The construction of such a map is critical for understanding molecular mechanisms that underlie viral infection and transmission processes for negative-sense RNA viruses like ADV, for which reverse genetic systems are not yet available (Min et al., 2010; Mann and Dietzgen, 2014). When direct bilateral protein–protein interactions were tested for ADV, one homotypic and three heterotypic interactions were detected, all involving the P protein (Fig. 4B).

The interaction of N and P proteins is a common feature among not only the already characterized LNYV (Martin et al., 2012), PYDV (Bandyopadhyay et al., 2010) and SYNV (Min et al., 2010) but also the recently characterized dichorhaviruses coffee ringspot virus (CoRSV) (Ramalho et al., 2014) and orchid fleck virus (OFV) (Kondo et al., 2013), which have bipartite, negative-strand RNA genomes with clear sequence similarities to those of nucleorhabdoviruses, and the vertebrate rhabdovirus, vesicular stomatitis virus (VSV) (Moerdyk-Schauwecker et al., 2009; Fig. 7b in Martin et al., 2012). In this study, interaction between ADV N and P was

also demonstrated by BiFC, where the location of the N:P complex was subnuclear, similar to that reported for SYNV, PYDV, CoRSV and OFV (Bandyopadhyay et al., 2010; Min et al., 2010; Kondo et al., 2013; Ramalho et al., 2014), but different to that observed for LNYV, which was in the cytoplasm (Martin et al., 2012). The BiFC results for ADV N and P proteins confirmed the earlier observed co-localization results for these proteins, and showed that the interaction was similar to that reported for these two proteins from nucleorhabdoviruses rather than cytorhabdoviruses. This supports the hypothesis that the N:P association in ADV may be required for formation of subnuclear viroplasms, similar to those interactions in the nucleorhabdovirus SYNV (Deng et al., 2007).

The self-interaction of P protein was also reported for SYNV (Min et al., 2010) and LNYV (Martin et al., 2012), however was not observed for PYDV (Bandyopadhyay et al., 2010). The subnuclear localization of the ADV P:P complex (Fig. 4B) resembles that of the sole expression of GFP-P, and is different to that observed for LNYV P (Martin et al.,2012) at the cell periphery (Martin et al., 2012) and both nuclear and cytoplasmic localization for SYNV P (Min et al., 2010).

This report shows for the first time an interaction between the putative movement protein P3 and the P protein of a plant rhabdovirus. Additional information was gained from co-expression of P and P3, which resulted in the relocalization of only some (P-interacting) P3 to the nucleus, while the majority of P3 remained at the cell periphery and did not co-localize with P protein. This may be an indication of multiple virus movement related functions of P3 by itself at the cell periphery and in a complex involving P protein in the nucleus. The P:P3 interaction is characterized by the re-localization of some P3 from the cell periphery to the nucleus. GST pull-down assays showed that RYSV P3 specifically binds to cognate N protein, indicating its involvement in cell-to-cell movement (Huang et al., 2005). On the other hand, the putative movement protein of PYDV was shown to interact with cognate M and G proteins (Bandyopadhyay et al., 2010), whereas SYNV sc4 interacts with the G protein (Min et al., 2010). Based on this data it was proposed that M and G proteins, in the case of PYDV (Bandyopadhyay et al., 2010), and G protein, for SYNV (Min et al., 2010), are involved (also including several host proteins) in the formation of movement complexes, respectively. Therefore, in the case of ADV one might predict that P protein may be involved in the formation of the movement complex. Furthermore, like for ADV, it has been observed for both PYDV and SYNV that the interactions with either M or G proteins result in relocalization of the movement proteins from the cell periphery to the nucleus, the site of viral replication and morphogenesis for these nucleorhabdoviruses (Bandyopadhyay et al., 2010; Min et al., 2010).

The interaction of M and P proteins has so far only been reported for the cytorhabdoviruses ADV and LNYV (Martin et al., 2012), but not for the nucleorhabdoviruses PYDV and SYNV (Bandyopadhyay et al., 2010; Min et al., 2010). However, this interaction occurred inside the nucleus in small aggregates for ADV, while the M:P complexes were localized in aggregates in the cytoplasm for LNYV (Martin et al., 2012). This suggests that LNYV P protein may be involved in the relocalization of M protein to the cytoplasm, where the viral core complex is thought be condensed by the M protein (Jackson et al., 2005). On the other hand, as was shown by both the co-expression and BiFC results, ADV P protein may cause the relocalization of M into the nucleus, which supports the hypothesis that the cell nucleus may be the focal point for ADV replication machinery and viroplasm establishment.

In summary, the ADV protein localization and interaction data indicate an association of this virus with the nucleus, whereas ADV particles appear to be associated with ER membranes of infected cells when viewed by EM of thin sections (Bejerman et al., 2011) and have a clear genome sequence similarity and evolutionary links exist with cytorhabdoviruses. More detailed electron microscopy studies and a reverse genetics system based on further developments of plant rhabdovirus minireplicons (Ganesan et al., 2013) will be needed to confirm the site(s) of ADV replication and morphogenesis.

Although the intracellular localization of viral protein interactions observed was different for ADV and LNYV, overall the protein interaction maps for these two cytorhabdoviruses appear similar with four interactions observed for each virus. For ADV, the exception is the lack of a detectable M:M interaction, which is otherwise conserved across plant rhabdoviruses studied so far (Bandyopadhyay et al., 2010; Martin et al., 2012; Min et al., 2010). It should be noted that both ADV BiFC constructs that failed to detect the M:M interaction, were successful in detecting the M:P interaction, suggesting that fusion of YFP reporter protein fragments to ADV M protein did not interfere with its BiFC interaction capability.

Interactions of rhabdovirus proteins with plant proteins have been demonstrated for SYNV (Min et al., 2010) and several host proteins were found associated with VSV virions (Moerdyk-Schauwecker et al., 2009), indicating involvement of host proteins in rhabdovirus replication. It is conceivable that host proteins that play a role in ADV replication may interact undetected with viral proteins during BiFC assays and thereby block the viral protein YFP fusions from interacting. This could explain the lack of detection in BiFC assays of some expected protein–protein interactions, like M:M or G:G seen for some other plant rhabdoviruses (Bandyopadhyay et al., 2010; Martin et al., 2012).

Little is known about the functions of cytorhabdovirus P proteins, besides the recently determined structure of the C-terminal domain of LNYV P and its local RNA silencing suppressor activity in plants (Martinez et al., 2013; Mann et al., 2015). It would be of particular interest to determine if P protein nuclear localization and interaction with N protein may also be a feature of other cytorhabdoviruses that are closely related to ADV, like PeVA and SCV. Furthermore, the study of ADV P mutants will be required to identify functional domains involved in the interaction with N protein, identify putative nuclear import and export signals and define the import pathways used, to reveal the genome replication processes of ADV.

In conclusion, this research has provided further evidence that plant rhabdoviruses across the currently recognized genera are diverse in genome organization, and viral protein localization and interactions. We have also shown that the observed localization and interactions of ADV proteins in plant cells are not in full agreement with the evolutionary relationships and taxonomical placement in the *Cytorhabdovirus* genus suggested by phylogenetic genome sequence analysis.

Methods

Virus source and RNA purification

Young symptomatic leaves were collected from alfalfa plants growing in the rural area of Manfredi (Córdoba province). Total RNA was extracted using Trizol (Invitrogen, CA, USA) following the manufacturer's instructions. The amount and quality of RNA were checked using a spectrophotometer (Nanodrop, Thermo Fisher Scientific, Waltham, MA, USA).

RT-PCR and cloning of amplicons

Total RNA was sent to Fasteris Life Sciences SA (Plan-les-Ouates, Switzerland), where the bands located between 21 and 30 bp were excised, purified, processed and sequenced on a Illumina HiSeq 2000. Raw data were processed using the pipeline ngs_backbone

1.4.0 (Blanca et al., 2011) to remove adapter barcode and low-quality regions. The cleaned reads were *de novo* assembled with the software package Velvet v0.6.04 (Zerbino and Birney, 2008) and the identity of individual contigs was analyzed using BLASTn and BLASTx. Short fragments of the N, G and L genes, assembled using Velvet, were used to design specific primers to amplify the complete viral genome. Complementary DNA was synthesized using M-MLV Reverse Transcriptase (Promega, Madison, USA) from total RNA and using ADV-specific primers. Five large fragments (5.3 kb, 3.2 kb, 1 kb, 1.2 kb and 1.1 kb) covering most of the ADV genome (Fig. 1A) were amplified using the Expand Long Template PCR System (Roche, Mannheim, Germany) and appropriate primer pairs. The total RNA was used to determine the viral 3′ and 5′ terminal sequences by RACE. For 5′RACE, cDNA synthesis, purification and dC-tailing were performed using the 5′RACE System for Rapid Amplification of cDNA Ends, v2.0 (Invitrogen) kit, according to protocols provided by the supplier. For 3′RACE, total RNA was polyadenylated using *Escherichia coli* Poly(A) Polymerase (NEB, Ipswich, USA). An oligo (dT) primer was used for cDNA synthesis from the poly(A) RNA, together with a virus-specific primer for PCR.

All amplicons were gel-purified using the Wizard SV Gel and PCR Clean-Up System (Promega) and ligated into pGEM-T Easy Vector (Promega). Each nucleotide was sequenced in both directions from at least three independent clones using the Sanger method at the Australian Genome Research Facility (AGRF, Brisbane) or Macrogen (Seoul, South Korea) with universal M13 forward and reverse primers and internal primers as required.

Sequence analysis

Sequences were compiled and analyzed using the Lasergene 10 software package (DNASTAR, Inc., Madison, Wi, USA). Percentage nucleotide (nt) and amino acid (aa) sequence identity of ADV with available cyto- and nucleorhabdovirus sequences was calculated by ClustalW (Thompson et al., 1994) and implemented in the BioEdit 7.0.9.0 software (Hall, 1999). Phylogenetic analysis of the aa sequence of the complete N protein and domain III of the L protein was carried out using neighbor-joining (NJ) and maximum likelihood (ML) methods, as implemented in MEGA 6.0 (Tamura et al., 2013).

Protein sequences were searched for domains and motifs, including transmembrane domains (TMHMM version 2.0 http://www.cbs.dtu.dk/services/TMHMM/) (Krogh et al., 2001), N-terminal signal peptides (SignalP version 4.1 http://www.cbs.dtu.dk/services/SignalP/) (Petersen et al., 2011), nuclear localization signals (NLSs) (cNLS Mapper) (Kosugi et al., 2009), nuclear export signals (NetNES 1.1) (La Cour et al., 2004) and glycosylation sites (PROSITE http://us.expasy.org/prosite/) (Sigrist et al., 2012).

Transient in planta protein expression and live cell imaging

Each ADV open reading frame (ORF), except that encoding the L protein, was amplified from total RNA of ADV-infected alfalfa using gene-specific primers that incorporated attB recombination sites. Complementary DNA was synthesized using First-strand Synthesis Supermix (Life Technologies, Carlsbad, USA) and random primers. Phusion High Fidelity proof-reading polymerase (Finnzymes, Waltham, USA) was used in PCR; amplicons were gel-purified and cloned into pDONR221 (Life Technologies) using BP clonase. Chemically-competent Omnimax *E. coli* were transformed using the heat shock method and recombinant colonies selected on Luria-Bertani (LB) agar containing 50 mg/L kanamycin. Plasmid DNA was extracted using the GeneJet plasmid purification kit (Thermo Scientific, Waltham, MA, USA) and cloned inserts were fully sequenced. Sequence-confirmed Gateway entry clones were recombined into pSITE destination vectors and used for the expression of autofluorescent protein fusions in plant cell for localization and bimolecular fluorescence complementation (BiFC) assays as described (Chakrabarty et al., 2007; Martin et al., 2009). Plant expression vectors used in this study were pSITE-2CA, pSITE-2NA (viral proteins fused to GFP C or N-terminus, respectively) for all proteins, pSITE-4CA (fusions to mRFP C-terminus) for N, P, P3 and M proteins for co-expression experiments, and pSITE-BiFC-nEYFP-C1 and pSITE-BiFC-cEYFP-C1 vectors for BiFC assays, where all viral proteins were tested as C-terminal fusions to the amino (nec) or carboxy (cec) terminal portions of YFP. Recombinant pSITE vectors were individually transformed into *Agrobacterium tumefaciens* LBA 4404 and suspensions infiltrated into *N. benthamiana* leaves as previously described (Tsai et al., 2005). To assist in the identification of intracellular structures, mCherry-ER marker plasmid (Nelson et al., 2007) was co-infiltrated into wildtype plants, or red fluorescent nuclei (RFP-Histone 2B) or cyan fluorescent nuclei (CFP-Histone 2B) transgenic marker plants (Martin et al., 2009) were used. Sections taken from at least three leaves from each of three independent experiments (nine leaves total) were examined 2–3 days post agroinfiltration. Confocal laser scanning microscopy was performed on a Zeiss LSM-700 microscope; images were acquired using Zen 2012 Lite software and exported as tiff or jpeg files.

Acknowledgments

We thank Michael M. Goodin (University of Kentucky) for pSITE vectors and *N. benthamiana* fluorescent marker lines and critical reading of the manuscript, Krin S. Mann for a critical read of the manuscript and the Queensland Alliance for Agriculture and Food Innovation for financial support. N.B. was supported by a post-doctoral fellowship from INTA (Grant 1029/2012), Argentina, and is a member of CONICET, the Scientific Research Council of Argentina.

Appendix A. Supporting information

Supplementary data associated with this article can be found in the online version at http://dx.doi.org/10.1016/j.virol.2015.05.001.

References

Ammar, E.-D., Tsai, C.-W., Whitfield, A.E., Redinbaugh, M.G., Hogenhout, S.A., 2009. Cellular and molecular aspects of rhabdovirus interactions with insect and plant hosts. Annu. Rev. Entomol. 54, 447–468.

Anderson, G., Wang, R., Bandyopadhyay, A., Goodin, M., 2012. The nucleocapsid protein of Potato yellow dwarf virus: protein interactions and nuclear import mediated by a non-canonical nuclear localization signal. Front. Plant Sci. 3, 14.

Bandyopadhyay, A., Kopperud, K., Anderson, G., Martin, K., Goodin, M., 2010. An integrated protein localization and interaction map for Potato yellow dwarf virus, type species of the genus *Nucleorhabdovirus*. Virology 402, 61–71.

Bejerman, N., Nome, C., Giolitti, F., de Breuil, S., Kitajima, E., Pérez Férnandez, J., Basigalup, D., Cornacchione, M., Lenardon, S., 2011. First report of a rhabdovirus infecting alfalfa in Argentina. Plant Dis. 95, 771.

Blanca, J.M., Pascual, L., Ziarsolo, P., Nuez, F., Cañizares, J., 2011. ngs_backbone: a pipeline for read cleaning, mapping and snp calling using next generation sequence. BMC Genomics 12, 285.

Bourhy, H., Cowley, J.A., Larrous, F., Holmes, E.C., Walker, P.J., 2005. Phylogenetic relationships among rhabdoviruses inferred using the L polymerase gene. J. Gen. Virol. 86, 2849–2858.

Chakrabarty, R., Banerjee, R., Chung, S.-M., Farman, M., Citovsky, V., Hogenhout, S.A., Tzfira, T., Goodin, M., 2007. pSITE vectors for stable integration or transient expression of autofluorescent protein fusions in plants: probing *Nicotiana benthamiana* – virus interactions. Mol. Plant Microbe Interact. 20, 740–750.

Citovsky, V., Lee, L.Y., Vyas, S., Glick, E., Chen, M.H., Vainstein, A., Gafni, Y., Gelvin, S.B., Tzfira, T., 2006. Subcellular localization of interacting proteins by bimolecular fluorescence complementation in planta. J. Mol. Biol. 362, 1120.

Cokol, M., Nair, R., Rost, B., 2000. Finding nuclear localization signals. EMBO Rep. 1, 411–415.

Deng, M., Bragg, J.N., Ruzin, S., Schichnes, D., King, D., Goodin, M.M., Jackson, A.O., 2007. Role of the Sonchus yellow net virus N protein in formation of nuclear viroplasms. J. Virol. 81, 5362–5374.
Dietzgen, R.G., Callaghan, B., Wetzel, T., Dale, J.L., 2006. Completion of the genome sequence of Lettuce necrotic yellows virus, type species of the genus Cytorhabdovirus. Virus Res. 118, 16–22.
Dietzgen, R.G., Calisher, C.H., Kurath, G., Kuzmin, I.V., Rodriguez, L.L., Stone, D.M., Tesh, R.B., Tordo, N., Walker, P.J., Wetzel, T., Whitfield, A.E., 2011. Family *Rhabdoviridae*. In: King, A.M.Q., Adams, M.J., Carstens, E.B., Lefkowitz, E.J. (Eds.), Virus Taxonomy, Ninth Report of the International Committee on Taxonomy of Viruses. Elsevier, Oxford, pp. 686–714.
Ganesan, U., Bragg, J.N., Deng, M., Marr, S., Lee, M.Y., Qian, S., Shi, M., Kappel, J., Peters, C., Lee, Y., Goodin, M.M., Dietzgen, R.G., Li, Z., Jackson, A.O., 2013. Construction of a *Sonchus yellow net virus* minireplicon: a step towards reverse genetic analysis of plant negative-strand RNA viruses. J. Virol. 87, 10598–10611.
Ghosh, D., Brooks, R.E., Wang, R., Lesnaw, J., Goodin, M.M., 2008. Cloning and subcellular localization of the phosphoprotein and nucleocapsid proteins of *Potato yellow dwarf virus*, type species of the genus *Nucleorhabdovirus*. Virus Res. 135, 26–35.
Goodin, M.M., Austin, J., Tobias, R., Fujita, M., Morales, C., Jackson, A.O., 2001. Interactions and nuclear import of the N and P proteins of Sonchus yellow net virus, a plant nucleorhabdovirus. J. Virol. 75, 9393–9406.
Goodin, M.M., Dietzgen, R.G., Schichnes, D., Ruzin, S., Jackson, A.O., 2002. pGD vectors: versatile tools for the expression of green and red fluorescent protein fusions in agroinfiltrated plant leaves. Plant J. 31, 375–383.
Goodin, M.M., Chakrabarty, R., Banerjee, R., Shelton, S., DeBolt, S., 2007. New gateways to discovery. Plant Physiol. 145, 1100–1109.
Guo, H., Song, X., Xie, C., Huo, Y., Zhang, F., Chen, X.Y., Geng, Y., Fang, R., 2013. Rice yellow stunt rhabdovirus protein 6 suppresses systemic RNA silencing by blocking RDR6-mediated secondary siRNA synthesis. Mol. Plant Microbe Interact. 26, 927–936.
Hall, T., 1999. BioEdit: a user-friendly biological sequence alignment editor and analysis program for Windows 95/98/NT. Nucl. Acids. Res. Symp. Ser. 41, 95–98.
Heaton, L.A., Hillman, B.I., Hunter, B.G., Zuidema, D., Jackson, A.O., 1989. Physical map of the genome of Sonchus yellow net virus, a plant rhabdovirus with six genes and conserved gene junction sequences. Proc. Natl. Acad. Sci. USA 86, 8665–8668.
Heim, F., Lot, H., Delecolle, B., Bassler, A., Krczal, G., Wetzel, T., 2008. Complete nucleotide sequence of a putative new cytorhabdovirus infecting lettuce. Arch. Virol. 153, 81–92.
Huang, Y., Zhao, H., Luo, Z., Chen, X., Fang, R.-X., 2003. Novel structure of the genome of Rice yellow stunt virus: identification of the gene 6-encoded virion protein. J. Gen. Virol. 84, 2259–2264.
Huang, Y.W., Geng, Y.F., Ying, X.B., Chen, X.Y., Fang, R.X., 2005. Identification of a movement protein of Rice yellow stunt rhabdovirus. J. Virol. 79, 2108–2114.
Ito, T., Suzaki, K., Nakano, M., 2013. Genetic characterization of novel putative rhabdovirus and dsRNA virus from Japanese persimmon. J. Gen. Virol. 94, 1917–1921.
Jackson, A.O., Dietzgen, R.G., Goodin, M.M., Bragg, J.N., Deng, M., 2005. Biology of plant rhabdoviruses. Annu. Rev. Phytopathol. 43, 623–660.
Kondo, H., Chiba, S., Andika, I.B., Maruyama, K., Tamada, T., Suzuki, N., 2013. Orchid fleck virus structural proteins N and P form intranuclear viroplasm-like structures in the absence of viral infection. J. Virol. 87, 7423–7434.
Krogh, A., Larsson, B., von Heijne, G., Sonnhammer, E.L.L., 2001. Predicting transmembrane protein topology with a hidden Markov model: application to complete genome. J. Mol. Biol. 305, 567–580.
Kosugi, S., Hasebe, M., Tomita, M., Yanagawa, H., 2009. Systematic identification of yeast cell cycle-dependent nucleocytoplasmic shuttling proteins by prediction of composite motifs. Proc. Natl. Acad. Sci. USA 106, 10171–10176.
Kumar, M., Raghava, G.P., 2009. Prediction of nuclear proteins using SVM and HMM models. BMC Bioinform. 10, 22.
Kuzmin, I.V., Novella, I.S., Dietzgen, R.G., Padhi, A., Rupprecht, C.E., 2009. The rhabdoviruses: biodiversity, phylogenetics, and evolution. Infect. Genet. Evol. 9, 541–553.
La Cour, T., Kiemer, L., Molgaard, A., Gupta, R., Skriver, K., Brunak, S., 2004. Analysis and prediction of leucine-rich nuclear export signals. Prot. Eng. Des. Sel. 17, 527–536.
Mann, K., Dietzgen, R.G., 2014. Plant rhabdoviruses: new insights and research needs in the interplay of negative-strand RNA viruses with plant and insect hosts. Arch. Virol. 159, 1889–1900.
Mann, K., Johnson, K.N., Dietzgen, R.G., 2015. Cytorhabdovirus phosphoprotein shows RNA silencing suppressor activity in plant, but not in insect cells. Virology 476, 413–418.
Martin, K., Kopperud, K., Chakrabarty, R., Banerjee, R., Brooks, R., Goodin, M.M., 2009. Transient expression in *Nicotiana benthamiana* fluorescent marker lines provides enhanced definition of protein localization, movement and interactions *in planta*. Plant J. 59, 150–162.
Martin, K.M., Dietzgen, R.G., Wang, R., Goodin, M.M., 2012. Lettuce necrotic yellows cytorhabdovirus protein localization and interaction map, and comparison with nucleorhabdoviruses. J. Gen. Virol. 93, 906–914.
Martinez, N., Ribeiro Jr., E.A., Leyrat, C., Tarbouriech, N., Ruigrok, R.W., Jamin, M., 2013. Structure of the C-terminal domain of Lettuce Necrotic Yellows Virus phosphoprotein. J. Virol. 87, 9569–9578.
Massah, A., Izadpanah, K., Afsharifar, A.R., 2008. Analysis of nucleotide sequence of Iranian maize mosaic virus confirms its identity as a distinct nucleorhabdovirus. Arch. Virol. 153, 1041–1047.
Mattaj, I.W., Englmeier, L., 1998. Nucleo cytoplasmic transport: the soluble phase. Annu. Rev. Biochem. 67, 265–306.
Min, B.E., Martin, K., Wang, R., Tafelmeyer, P., Bridges, M., Goodin, M., 2010. A host-factor interaction and localization map for a plant-adapted rhabdovirus implicates cytoplasm-tethered transcription activators in cell-to-cell movement. Mol Plant Microbe Interact. 23, 1420–1432.
Moerdyk-Schauwecker, M., Hwang, S.I., Grdzelishvili, V.Z., 2009. Analysis of virion associated host proteins in vesicular stomatitis virus using a proteomics approach. Virol. J. 6, 166.
Nelson, B.K., Cai, X., Nebenführ, A., 2007. A multicolored set of in vivo organelle markers for co-localization in Arabidopsis and other plants. Plant J. 51, 1126–1136.
Pappi, P.G., Dovas, C.I., Efthimiou, K.E., Maliogka, V.I., Katis, N.I., 2013. A novel strategy for the determination of a rhabdovirus genome and its application to sequencing of Eggplant mottled dwarf virus. Virus Genes 47, 105–113.
Petersen, T.M., Brunak, S., von Heijne, G., Nielsen, H., 2011. SignalP 4.0: discriminating signal peptides from transmembrane regions. Nat. Methods 8, 785–786.
Ramalho, T.O., Figueira, A.R., Sotero, A.J., Wang, R., Geraldino Duarte, P.S., Farman, M., Goodin, M.M., 2014. Characterization of Coffee ringspot virus-Lavras: a model for an emerging threat to coffee production and quality. Virology 464–465, 385–396.
Redinbaugh, M.G., Hogenhout, S.A., 2005. Plant rhabdoviruses. Curr. Top. Microbiol. Immunol. 292, 143–163.
Reed, S.E., Tsai, C.W., Willie, K.J., Redinbaugh, M.G., Hogenhout, S.A., 2005. Shotgun sequencing of the negative-sense RNA genome of the rhabdovirus Maize mosaic virus. J. Virol. Methods 129, 91–96.
Revill, P., Trinh, X., Dale, J.L., Harding, R., 2005. Taro vein chlorosis virus: characterization and variability of a new nucleorhabdovirus. J. Gen. Virol. 86, 491–499.
Schoen, C.D., Limpens, W., Moller, I., Groeneveld, L., Klerks, M.M., Lindner, J.L., 2004. The complete gnomic sequence of Strawberry crinkle virus, a member of the Rhabdoviridae. Acta Hortic. 656, 45–50.
Sigrist, C.J.A., de Castro, E., Cerutti, L., Cuché, B.A., Hulo, N., Bridge, A., Bougueleret, L., Xenarios, I., 2012. New and continuing developments at PROSITE. Nucleic Acids Res. 41, 344–347.
Tamura, K., Stecher, G., Peterson, D., Filipsli, A., Kumar, S., 2013. MEGA6: molecular evolutionary genetics analysis version 6.0. Mol. Biol. Evol. 30, 2725–2729.
Tanno, F., Nakatsu, A., Toriyama, S., Kojima, M., 2000. Complete nucleotide sequence of Northern cereal mosaic virus and its genome organization. Arch. Virol. 145, 1373–1384.
Thompson, J.D., Higgins, D.G., Gibson, T.J., 1994. CLUSTALW: improving the sensitivity of progressive multiple sequence alignment through sequence weighting, position-specific gap penalties and weight matrix choice. Nucleic Acids Res. 22, 4673–4680.
Trucco, V., de Breuil, S., Bejerman, N., Lenardon, S., Giolitti, F., 2014. Complete nucleotide sequence of Alfalfa mosaic virus isolated from alfalfa (*Medicago sativa* L.) in Argentina. Virus Genes 48, 562–565.
Tsai, C.-W., Redinbaugh, M.G., Willie, K.J., Reed, S., Goodin, M., Hogenhout, S.A., 2005. Complete genome sequence and in planta subcellular localization of Maize fine streak virus proteins. J. Virol. 79, 5304–5314.
Walker, P.J., Dietzgen, R.G., Joubert, D.A., Blasdell, K.R., 2011. Rhabdovirus accessory genes. Virus Res. 162, 110–125.
Yan, T., Zhu, J.-R., Di, D., Gao, Q., Zhang, Y., Zhang, A., Yan, C., Miao, H., Wang, X.-B., 2015. Characterization of the complete genome of Barley yellow striate mosaic virus reveals a nested gene encoding a small hydrophobic protein. Virology 478, 112–122. http://dx.doi.org/10.1016/j.virol.2014.12.042.
Zerbino, D.R., Birney, E., 2008. Velvet: algorithms for de novo short read assembly using de Bruijn graphs. Genome Res. 18, 821–829.